MCB
Journals.ASM.org

Protein Tyrosine Phosphatase-Like A Regulates Myoblast Proliferation and Differentiation through MyoG and the Cell Cycling Signaling Pathway

Xi Lin,[a] Xiangsheng Yang,[a] Qi Li,[b] Yanlin Ma,[b] Shuang Cui,[c] Dacheng He,[c] Xia Lin,[d] Robert J. Schwartz,[e] and Jiang Chang[a,b]

Texas A&M Health Science Center, Institute of Biosciences and Technology, Houston, Texas, USA[a]; Hainan Provincial Key Laboratory for Human Reproductive Medicine and Genetic Research, Affiliated Hospital of Hainan Medical College, Hainan, China[b]; Beijing Normal University, Beijing, China[c]; Surgery/General Surgery Division, Baylor College of Medicine, Houston, Texas, USA[d]; and Biology and Biochemistry Department, University of Houston, Houston, Texas, USA[e]

Protein tyrosine phosphatase-like A (PTPLa) has been implicated in skeletal myogenesis and cardiogenesis. Mutations in PTPLa correlated with arrhythmogenic right ventricular dysplasia in humans and congenital centronuclear myopathy with severe hypotonia in dogs. The molecular mechanisms of PTPLa in myogenesis are unknown. In this report, we demonstrate that PTPLa is required for myoblast growth and differentiation. The cells lacking PTPLa remained immature and failed to differentiate into mature myotubes. The repressed MyoG expression was responsible for the impaired myoblast differentiation. Meanwhile, impeded cell growth, with an obvious S-phase arrest and compromised G_2/M transition, was observed in PTPLa-deficient myoblasts. Further study demonstrated that the upregulation of cyclin D1 and cyclin E2 complexes, along with a compromised G_2/M transition due to the decreased CDK1 (cyclin-dependent kinase 1) activity and upregulated p21, contributed to the mutant cell S-phase arrest and eventually led to the retarded cell growth. Finally, the transcriptional regulation of the PTPLa gene was explored. We identified PTPLa as a new target gene of the serum response factor (SRF). Skeletal- and cardiac-muscle-specific SRF knockouts resulted in significant decreases in PTPLa expression, suggesting a conserved transcriptional regulation of the PTPLa gene in mice.

Skeletal myogenesis involves multiple processes in which undifferentiated myoblasts proliferate, withdraw from the cell cycle, and differentiate into mononucleated myocytes followed by a subsequent fusion of myocytes into multinucleated myotubes. The latter are assembled into mature muscle fibers along with the expression of muscle-specific proteins. The multistep process is tightly regulated in order to secure normal myogenesis development. Extensive studies that have focused on myogenic transcriptional regulation revealed four essential myogenic regulatory factors (MRFs), MyoD (17), MyoG (myogenin) (20, 65), Myf5 (muscle regulatory factor 5) (11), and MRF4 (muscle regulatory factor 4) (10, 47, 55). These factors function coordinately at different stages of muscle cell fate during development and play crucial roles in myogenesis. In comparison with myogenic transcriptional regulation, there have been far fewer studies of posttranslational regulation of myogenesis. Accumulating evidence has begun to reveal that tyrosyl phosphorylation and its opposite, dephosphorylation, are important regulatory components during myogenic progression. Several representative studies have examined focal adhesion kinase (FAK), a nonreceptor tyrosine kinase also known as protein tyrosine kinase 2 (53, 54), phosphatidylinositol 3′-kinase (PI3K) (16, 30), phosphoinositide phosphatase myotubularin, and protein tyrosine phosphatase SHP-2 (22, 32, 33).

Protein tyrosine phosphatase-like A (PTPLa) is a protein tyrosine phosphatase in which the active motif (I/V)HCXXGXX**P** (S/T) contains an arginine-to-proline replacement (indicated by boldface) (61). While the significance of this substitution remains to be determined, the developmental expression and specific tissue distribution of the mouse PTPLa transcripts strongly imply a role in skeletal myogenesis and cardiogenesis. In mouse embryos, PTPLa expression in somites throughout myogenesis and in cardiomyocytes of the primitive heart was detected by *in situ* hybridization as early as embryonic day 8.5 (E8.5) (61). Consistent with the embryonic expression pattern, the highest transcript levels of PTPLa were observed in adult mouse heart and skeletal muscle (61). However, the biological function of PTPLa in muscle development remains largely unknown. Mutations in the PTPLa gene were found in patients suffering from arrhythmogenic right ventricular dysplasia (ARVD) (31, 38) and in Labrador retrievers suffering from congenital myopathy (52), suggesting a potential role of PTPLa in muscle development and normal function.

In this study, we assessed PTPLa protein levels in adult mouse tissues and found that PTPLa was almost exclusively expressed in heart and skeletal muscle. We then used C2C12 myoblasts as a tool to study PTPLa's effect on myoblast proliferation and differentiation and the associated molecular mechanism by gain- and loss-of-function approaches. Our data provide evidence that PTPLa is an important regulator in skeletal myogenesis. The promyogenic role of PTPLa is associated with the modulation of myogenic differentiation and proliferation, and PTPLa deficiency impedes both processes. Furthermore, we explored PTPLa transcriptional regulation and identified SRF (serum response factor) as a major transcription factor responsible for PTPLa gene expression.

Received 20 September 2011 **Returned for modification** 11 October 2011
Accepted 9 November 2011
Published ahead of print 21 November 2011
Address correspondence to Jiang Chang, jchang@ibt.tamhsc.edu.

doi:10.1128/MCB.05484-11

MATERIALS AND METHODS

Cell culture and plasmid constructs. C2C12 mouse myoblasts were cultured in either growth medium (GM) or differentiation medium (DM). The GM, which consisted of Dulbecco's modified Eagle's medium (DMEM) and 20% fetal bovine serum (FBS), was used to grow the C2C12 myoblasts and keep them from differentiation. For differentiation experiments, the cells were cultured in DM that contained DMEM and 2% heat-inactivated horse serum. Cell synchronization at G_0 was achieved by culturing cells in 1% FBS for 24 h. For double-thymidine synchronization, cells were treated with 1 mM thymidine for 12 h followed by a 10-h break and were then treated again with the same dose of thymidine for another 12 h before the blockage release.

The mouse PTPLa cDNA was cloned from a wild-type C57 mouse heart cDNA template by PCR. The PCR primers designed based on the mouse PTPLa mRNA sequence (NCBI accession no. NM_013935) were 5′-ATGCCGCTCGAGCTCCTGTGCGCTGCTCCT-3′ (forward) and 5′-ATGCCGGAATTCGCACCTTGTGTGTGGGAAC-3′ (reverse). The PTPLa cDNA was cloned into the pcDNA3.1/myc-his(−) B (Invitrogen) with a green fluorescent protein (GFP) tag at the C terminus. SRF expression vector was generated as previously described (14). The human MyoG-expressing plasmid was from OriGene.

Generation of PTPLa and MyoG-deficient myoblast cell lines. Lentiviral vectors V2LHS_5923, and V2LMM_6871 (Thermo Scientific) expressing short hairpin RNAs (shRNAs) specific for mouse PTPLa and MyoG, respectively, were used to generate recombinant lentiviruses for myoblast infection to establish cell lines. Vector expressing nonsilencing shRNA (RHS4346) was used as a control. Briefly, the 293FT (Invitrogen, Carlsbad, CA) cells were transfected with the lentiviral vector expressing specific shRNA with two helper vectors, pMD2.G and psPAX2, to produce the lentivirus. C2C12 myoblasts were then infected with the virus at an MOI (multiplicity of infection) of 10 with Polybrene (8 μg/ml) to enhance the virus transduction. The viral infection was monitored by following GFP expression. The stable cell lines were established by selection with puromycin (10 μg/ml).

Immunostaining and immunoblotting. Cells on a glass coverslip were briefly fixed using 4% paraformaldehyde and permeabilized using phosphate-buffered saline containing 10% FBS and 0.2% Triton X-100. The cells were then treated with a blocking solution, phosphate-buffered saline with 5% BSA and 0.1% Triton X-100, before incubations with antibodies were performed. The primary anti-myosin heavy chain (anti-MHC) antibody (MF-20; Developmental Studies Hybridoma Bank) and the secondary goat anti-mouse IgG antibody coupled with Alexa Fluor 594 (Invitrogen, Carlsbad, CA) were used. Nuclei were visualized by DAPI (4′,6′diamidino-2-phenylindole) staining (Vectashield, Vector Laboratories, Inc.), and images were acquired by fluorescence microscopy. Myoblast morphological differentiation images were taken using phase-contrast microscopy. Protein samples for Western blot analysis were extracted and separated as described previously (13). Antibodies against PTPLa, MyoG, and p21 were from Bethyl Laboratory, Inc., Santa Cruz Biotechnology, and Cell Signaling, respectively. Equivalent protein loadings were verified and normalized according to the intensities of GAPDH (glyceraldehyde-3-phosphate dehydrogenase) blots.

QPCR analysis. Transcripts were quantified by quantitative PCR (QPCR) analysis (Stratagene Mx3000p qPCR system) using the SYBR green method with a MasterMix buffer system containing *Taq* polymerase (Stratagene) as described previously (39). Total RNAs was prepared by TRIzol extraction (Gibco BRL). The forward/reverse PCR primers (5′ to 3′) were as follows: for PTPLa (NM_013935), CCGGGTGGTTGGTTCTTGCTATT/GCGGCAAGTGGTCGAGGAGA; for MyoG (NM_031189), TGGAGCTGTATGAGACATCCC/TGGACAATGCTCAGGGGTCCC; for Acta-1 (NM_009606), AGACACCATGTGCGACGAAGA/TGCAGACCTTCGATGTAGCGGAT; for TnC (NM_009394), TTTGGGTGGTGGAGTGCGGAGGAGA/GTCACAGAGCCCAAAGGAGCAGCCTT; for myh3 (NM_001099635), TGAAGAAGGAGCAGGACACCAG/CACTTGGAGTTTATCCACCAGATCC; for myh8 (NM_177369), AACTGAGGAAGACCGCAAGAATG/AAGTAAACCCAGAGAGGCAAGTGACC; for MyoD (NM_010866), GCAGGCTCTGCTGCGCGACC/TGCAGTCGATCTCTCAAAGCACC; for Myf5 (NM_008656), TGCCATCCGCTACATTGAGAG/CCGGGGTAGCAGGCTGTGAGTTG; and for Myf6 (NM_008657), CTGCGCGAAAGGAGGAGACTAAAG/ATGGAAGAAAGGCGCTGAAGACTG. GAPDH expression levels were used for QPCR normalization. Expression levels were determined by the $2^{-\Delta\Delta Ct}$ threshold cycle method.

BrdU staining, FACS with propidium iodide (PI) staining, and M-phase assessment. Cells were synchronized and then cultured in GM for 12 h followed by BrdU (bromodeoxyuridine) treatment for 45 min before harvesting. The anti-BrdU antibody and the corresponding second antibody were purchased from Invitrogen (Zymed's BrdU kit). Single-cell suspensions containing at least 1×10^6 synchronized cells grown in GM were prepared for the cell cycle analyses by FACS (fluorescence-activated cell sorting) using a FACSCalibur system (Becton Dickinson Biosciences, San Diego, CA) (28). The data were processed using ModFit LTTM software (Verity Software House, Inc., Topsham, ME) to determine cell populations in the G_0/G_1, S, and G_2/M phases. To further assess the cell population in M phase, the synchronized cells were cultured in a serum restoration growth medium for 0, 4 and 8 h. Cell nuclei were visualized by DAPI staining. Five random images were taken using a 20× florescent microscopy objective. Cells showing typical telophase morphology (double nuclei) were counted as M phase positive. The percentage of M-phase population was calculated by comparing the number of M-phase-positive cells to total nuclei.

Electrophoretic mobility shift assay (EMSA). The ^{32}P-labeled 19- to 20-bp-long DNA duplexes containing the individual serum response elements (SREs) from the 5-kb region upstream of the PTPLa gene were used as probes, and the control SRE-positive probe was derived from a skeletal α-actin promoter containing one SRE (14). Mutant SRE probes were used to validate the specificity of binding. The probes (5′ to 3′) were as follows: for SRE1, TTGTTCCTCCTATGGGGCT/AGCCCCATAGGAGGAACAA; for SRE2, TAGCTCCTTCTCTGGGGACC/GGTCCCCAGAGAAGGAGCTA; for SRE3, ACATCCATAAAAGGAAAGA/TCTTTCCTTTTATGGATGT; and for the mutant SRE3, ACATAAATAAAAAAAAAGA/TCTTTTTTTTTATTTATGT. Experiments examining the supershift by the anti-SRF antibody and competition with unlabeled probe were conducted to verify the SRF-DNA interaction as described previously (59). Nuclear extracts were used for each experiment.

Luciferase assay. The 5-kb region upstream of the PTPLa gene containing the SRE3 site was subcloned into pGL3-basic vector expressing a luciferase reporter gene (Promega). A similar vector with the SRE3 mutant was constructed as a mutant reporter vector. Generation of the SRF expression vector and transient transfections were described previously (14). The luciferase assay was conducted 36 h posttransfection. Lysis buffer was purchased from Promega (E3971), and 20 of 60 μl of the lysis supernatant was used with a Monolight 3010 luminometer (Pharmingen) for the measurement of luciferase activity. Each sample was measured three times. All results were normalized to β-galactosidase activity (MRX Revelation; DYNEX Technologies).

Chromatin immunoprecipitation (ChIP) assay. The SRF expression vector was transfected into C2C12 cells. After 36 h, cells were gently fixed with formaldehyde and lysed by sonication. The specific SRF-DNA complex was immunoprecipitated using anti-SRF antibody. The identity of the DNA fragments isolated in the complex with SRF was determined by PCR, and the final PCR products were then sequenced to confirm the presence of the SRE motif.

Generation of skeletal- and cardiac-muscle-specific SRF knockout mice. Constitative SRF knockout resulted in early embryonic lethality due to several defects in mesoderm formation (4). To avoid the lethality and evaluate the PTPLa expression level under SRF-null conditions, $SRF^{loxp/loxp}$ mice (a generous gift from Alfred Nordheim) were bred with αMHC-MerCreMer and MCK-Cre mice (Jackson Laboratory) to generate $SRF^{loxp/loxp/Mer\text{-}CreMer}$ and $SRF^{loxp/loxp/MCK\text{-}Cre}$ mice, respectively. SRF deletion in cardiomyocytes was achieved by application

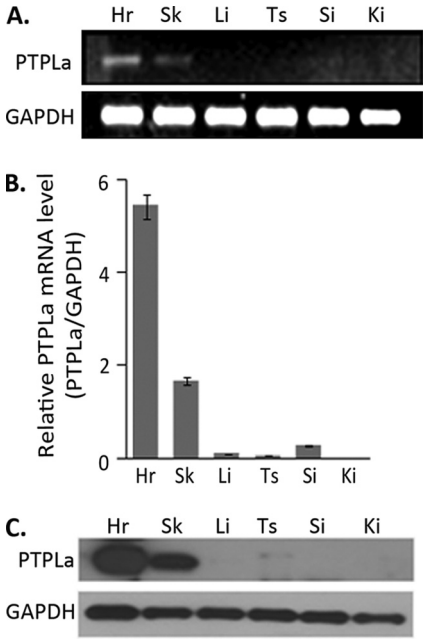

FIG 1 PTPLa tissue expression profile. (A) PTPLa expression levels in different adult mouse tissues were assessed by RT-PCR. (B) QPCR (the data represent the averages of three measurements with means ± standard errors). (C) Western blot analysis. The highest expression level of PTPLa was found in heart followed by skeletal muscle. PTPLa expression was undetectable in the rest of the tissues, except a trace of PTPLa protein was detected in testis tissue. Hr, heart; Sk, skeletal muscle; Li, liver; Ts, testis; Si, small intestine; Ki, kidney; GAPDH, glyceraldehyde-3-phosphate dehydrogenase. Samples in each tissue category from four animals were used for QPCR analysis.

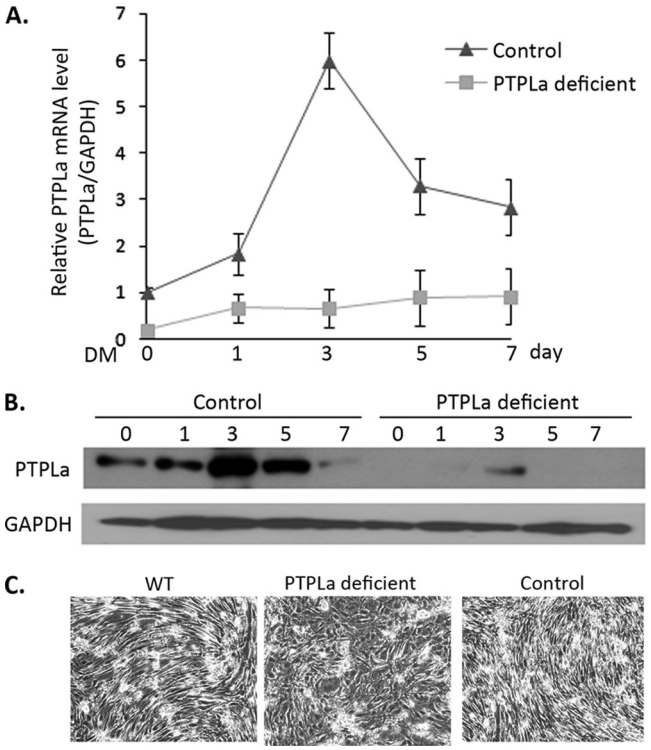

FIG 2 Upregulated PTPLa expression during myoblast differentiation and impaired myogenesis when PTPLa is lacking. (A) Myoblast differentiation was induced by DM (differentiation medium), and a marked transcript increase in the PTPLa level was detected by a QPCR assay. The upregulated PTPLa expression was totally abolished in PTPLa-deficient myoblasts. The time point data represent the averages of the results of three measurements (means ± standard errors). (B) The change in PTPLa protein level was assessed by the Western blot analysis. (C) The mutant myoblasts failed to differentiate, showed no myotube formation, and retained the proliferating morphology changes. The images were taken after 3 days of culture in DM. WT, wild type.

of tamoxifen (20 μg/g of body weight; intraperitoneal injection for 4 days) (57). All experiments with animals were approved by the Institutional Animal Care and Use Committee of the Texas A&M Health Science Center—Houston.

Statistical analysis. Data were expressed as means ± standard errors of the means. In multiple comparisons, one-way analysis of variance (ANOVA) was used followed by the Holm-Sidak method. In two-group comparisons, a nonpaired *t* test was used (SigmaPlot, version 11.0). A value of $P < 0.05$ was considered significant.

RESULTS

PTPLa is highly expressed in cardiac and skeletal muscle. To explore the biological functions of PTPLa, we evaluated the PTPLa expression profile in six different adult mouse tissues. The highest expression level of PTPLa mRNA was observed in the heart followed by skeletal muscle (Fig. 1). The transcription level of PTPLa was assessed by regular PCR (Fig. 1A) and quantified by QPCR analysis (Fig. 1B). The PTPLa mRNA level in the heart was more than 2-fold higher than in skeletal muscle (Fig. 1B). PTPLa mRNA was undetectable in the rest of the tissues. A similar observation was made for PTPLa protein expression assessed by Western blot analysis (Fig. 1C). The PTPLa protein expression was detected in both mouse heart and skeletal muscle, with the highest level in the heart (Fig. 1C). A trace PTPLa protein was detected in testis but not in other tissues.

PTPLa is upregulated during myoblast differentiation, and the differentiation is impaired in the presence of PTPLa deficiency. Since PTPLa is highly expressed in cardiac and skeletal muscles, we used the loss- and gain-of-function approaches to focus on PTPLa's role in skeletal myogenesis in C2C12 myoblasts. The PTPLa-deficient myoblast cell line was established by the use of lentivirus-expressing PTPLa-specific shRNA. The myoblast differentiation was then induced in both the control (nonspecific-shRNA-treated myoblasts) and PTPLa-deficient myoblast cells by serum deprivation (differentiation medium [DM]), and the PTPLa transcript and protein levels were assessed by QPCR (Fig. 2A) and Western blot analysis (Fig. 2B). We observed that the PTPLa mRNA level gradually increased to the peak value at differentiation day 3 in control myoblasts and then returned to the basic level. The dynamic change in PTPLa expression during differentiation was completely blocked in PTPLa-deficient myoblasts. Typical myoblast differentiation morphology changes, with cell elongation and alignment, cell fusion, and myotube formation, were observed in the wild-type and control myoblasts (Fig. 2C, left and right panels, respectively). However, the myoblasts lacking PTPLa failed to differentiate and retained the proliferating status (Fig. 2C, middle panel). This result implied a potential role of PTPLa in myoblast terminal differentiation and myotube formation.

To determine whether PTPLa is essential for myogenesis, the expression of several myogenic markers was monitored during myoblast differentiation. Significant increases in transcription of Acta-1 (skeletal α-actin), TnC (troponin C), Myh3 (embryonic skeletal myosin heavy chain 3), and Myh8 (perinatal skeletal

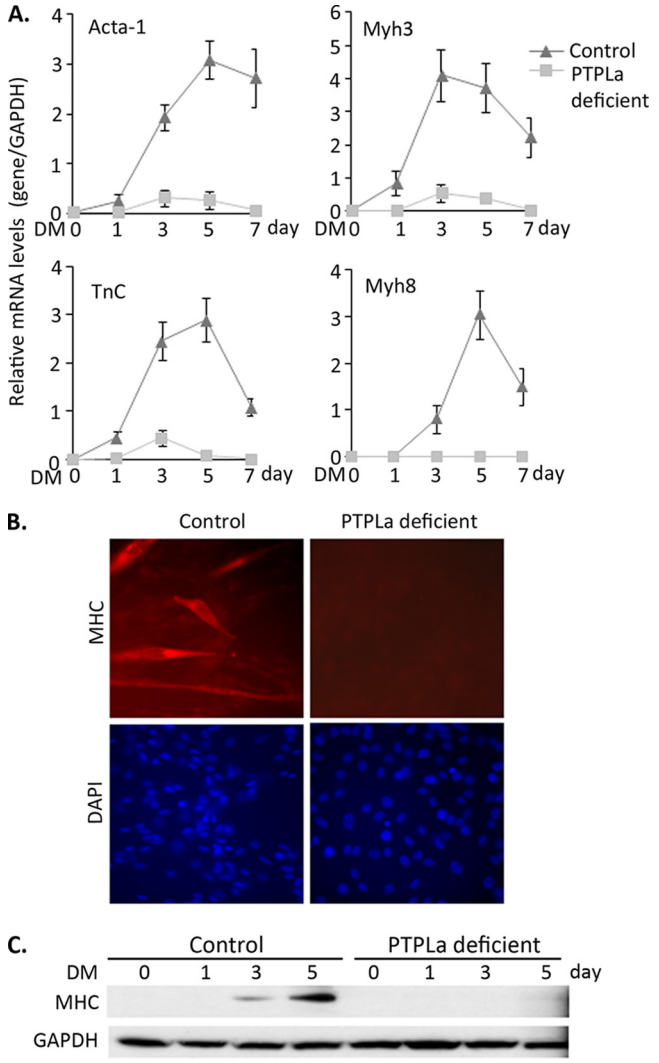

FIG 3 PTPLa-deficient myoblasts failed to express myogenic markers. (A) The induction of Acta-1, Myh3, TnC, and Myh8 transcripts was evaluated by QPCR, and upregulation of these myogenic markers was abolished in PTPLa-deficient myoblasts. The time point data represent the averages of the results of three measurements (means ± standard errors). (B) MHC expression and myotube formation were observed in control myoblasts but not in the mutant myoblasts by immunostaining. (C) The level of MHC protein was assessed by Western blot analysis, and no MHC protein was detected in the mutant myoblasts.

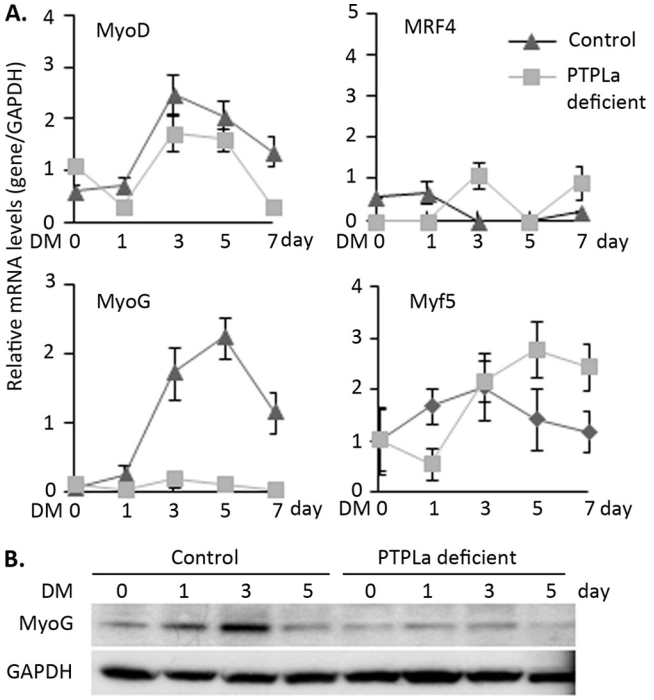

FIG 4 Impaired MyoG expression in PTPLa-deficient myoblasts. Four major skeletal myogenic regulatory factors were assessed during myoblast differentiation by QPCR (A), and no upregulation of MyoG transcripts and protein was observed in the mutant myoblasts (A and B). The time point data in panel A represent the averages of the results of three measurements (means ± standard errors).

myosin heavy chain 8) were detected in the control myoblasts by QPCR analysis, and the increases were impeded in the PTPLa-deficient myoblasts (Fig. 3A). The myotube formation was observed along with an induction of MHC (myosin heavy chain) expression in the control myoblasts but not in the PTPLa-deficient myoblasts (Fig. 3B). The Western blot result for MHC protein expression was consistent with the immunohistochemistry observation (Fig. 3C), showing a lack of MHC protein induction in PTPLa-deficient myoblasts. Together, these data indicated that myogenesis was impaired by a loss of PTPLa in C2C12 myoblasts.

PTPLa regulates myogenesis through MyoG. Skeletal muscle differentiation is tightly regulated by basic helix-loop-helix myogenic regulatory factors (MRFs) MyoD, Myf5, MyoG, and MRF4 (1–3, 6, 9). These factors function as master regulators in skeletal muscle development. To evaluate their roles in PTPLa-mediated myoblast differentiation, we analyzed expression of these four skeletal-muscle-specific regulatory factors by QPCR during myoblast differentiation. A marked increase in MyoG mRNA levels was observed in control myoblasts; however, the deficiency of PTPLa completely impeded the MyoG increase (Fig. 4A). The repressed MyoG protein expression in the mutant myoblasts was observed by the Western blot analysis (Fig. 4B). No significant differences between the control and PTPLa-deficient myoblasts in MyoD, Myf5, and MRF4 expression levels were found (Fig. 4A). This result implicated MyoG as a potential myogenic regulator in PTPLa-mediated myoblast differentiation.

To define the role of MyoG in PTPLa-mediated myoblast differentiation, a myoblast cell line lacking MyoG expression was generated. Two cell lines, the PTPLa-deficient and MyoG-deficient myoblasts, were used to test the hypothesis that PTPLa-mediated myoblast differentiation was induced through MyoG regulation. The plasmids expressing PTPLa and MyoG were transfected into the two mutant myoblasts, and the cell morphology changes, as well as levels of myogenic markers Acta-1 and MHC, were assessed (Fig. 5). After transfection with the PTPLa expression vector, PTPLa-deficient myoblasts resumed the differentiation morphology changes, with cell elongation and alignment and myotube formation. The differentiation resumption was observed in PTPLa-deficient myoblasts transfected with MyoG expression vector as well (Fig. 5A, upper panels). In the MyoG-deficient myoblasts, however, the cells resumed differentiation morphology changes only after MyoG expression vector transfection and not

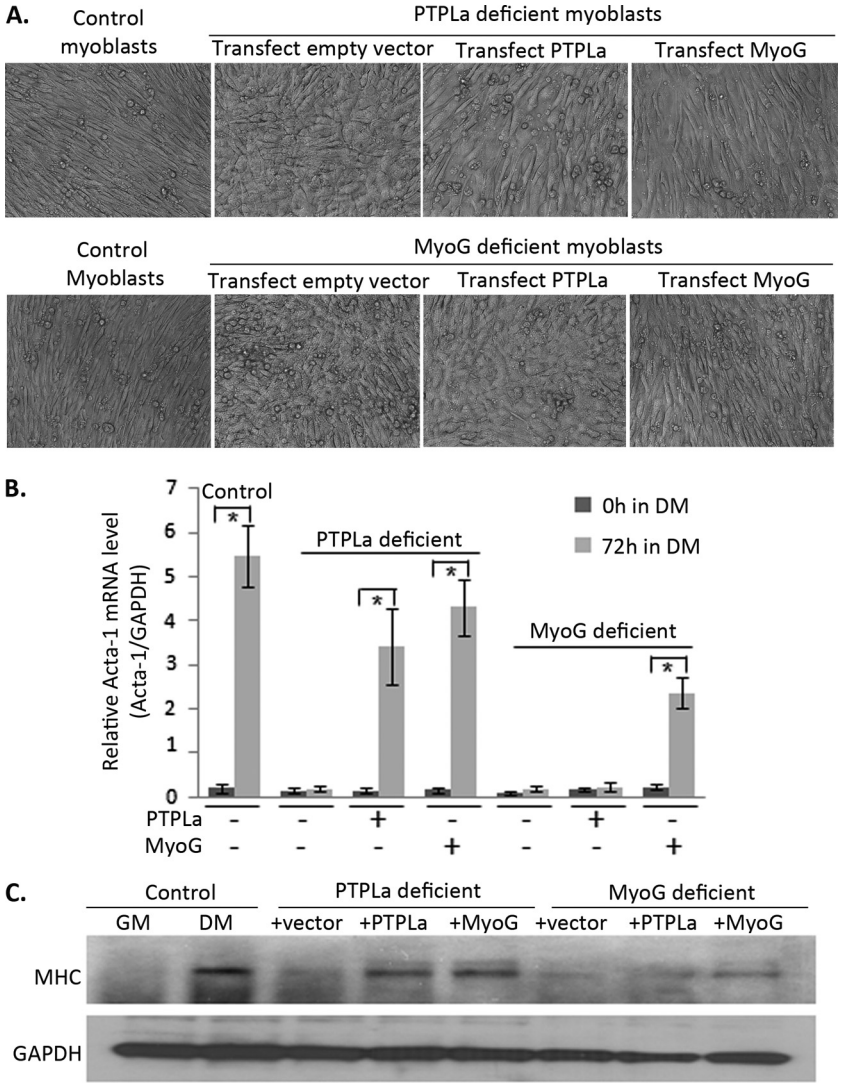

FIG 5 Impaired myogenesis in PTPLa-deficient myoblasts was rescued by MyoG. (A) Morphological changes of PTPLa-deficient and MyoG-deficient myoblasts after introduction of PTPLa and MyoG. The disrupted myotube formation observed in PTPLa mutant myoblasts was rescued by reintroducing MyoG or PTPLa (top panels). The impaired myogenesis in MyoG-deficient myoblasts was rescued only by reintroducing MyoG but not PTPLa (lower panels). (B) QPCR analysis of myogenic marker Acta-1 transcript levels in PTPLa and MyoG mutant myoblasts after introduction of PTPLa and MyoG. *, $P < 0.01$ compared to h 0 in DM. The time point data represent the averages of the results of three measurements (means ± standard errors). (C) Western blot analysis of the protein expression levels for another myogenic marker, MHC, in PTPLa and MyoG mutant myoblasts after introduction of PTPLa and MyoG.

after PTPLa expression vector transfection (Fig. 5A, lower panels), suggesting that MyoG may function downstream of PTPLa. This suggestion was supported by the QPCR and Western blot evaluation of expression levels for myogenic markers Acta-1 and MHC. The inductions of Acta-1 transcript and MHC protein were impeded in PTPLa-deficient as well as in MyoG-deficient myoblasts. Reintroduction of PTPLa or MyoG rescued Acta-1 and MHC expression in PTPLa-deficient myoblasts. However, in MyoG-deficient myoblasts, Acta-1 and MHC expression was rescued only by MyoG transfection and not by PTPLa transfection. Together, these data demonstrated that, as a transcriptional regulator downstream of PTPLa, MyoG was responsible for PTPLa-mediated myoblast differentiation.

Myoblast proliferation was impeded by PTPLa deficiency. In the study of PTPLa's role in myogenesis, we observed that myoblasts lacking PTPLa grew much slower in the growth medium than control myoblasts. To quantify the growth retardation, equal amounts of PTPLa-deficient and control myoblasts were synchronized and cultured in the growth medium to assess the cell growth rate differences. As shown in Fig. 6A, there were significantly smaller amounts of cells in the PTPLa-deficient group than in the control group. This gap in cell numbers was augmented at later times as cells grew exponentially. Meanwhile, the impeded cell proliferation in PTPLa-deficient myoblasts was confirmed by BrdU pulse-labeling at the 12-h time point. The number of BrdU-positive cells in the PTPLa-deficient group was about half of the control level, suggesting a proliferation defect in PTPLa-deficient myoblasts (Fig. 6B and C).

PTPLa knockdown resulted in S-phase arrest and compromised G_2/M transition in myoblasts. To study the mechanism of

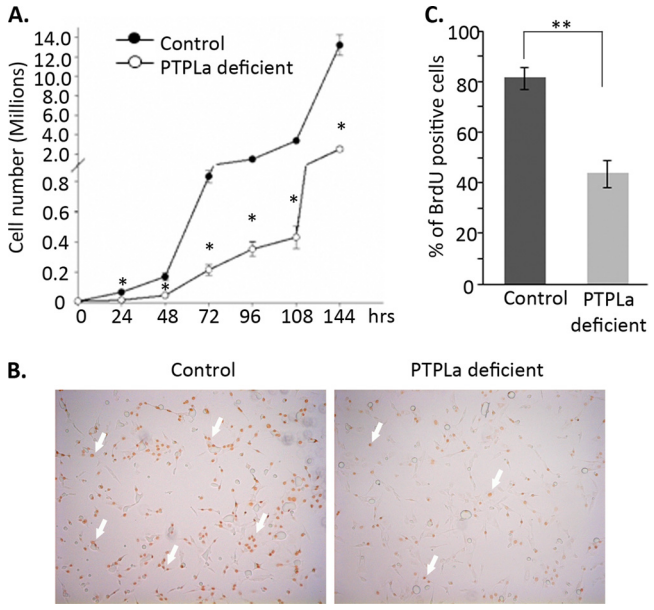

FIG 6 Myoblast proliferation was impeded by PTPLa deficiency. Cells were synchronized and cultured in the growth medium to assess the cell growth rate. (A and B) A retarded growth rate was observed (A), with fewer BrdU-stained cells in PTPLa mutant myoblasts (B). Brown, positive BrdU staining. Arrows indicate representative BrdU-positive cells. The panel A time point data represent the averages of the results of three measurements. (C) Quantitative analysis of BrdU staining. BrdU-positive cells were quantified from nine images taken from three slides at the 12-h time point. Data represent means ± standard errors. *, $P < 0.01$ compared to 0 h time point; **, $P < 0.01$ compared to control.

myoblast proliferation regulated by PTPLa, we evaluated the time dependence of the PTPLa effect on cell cycle progression. Synchronized (by low serum) myoblasts under subconfluent culture conditions were labeled with PI and analyzed by DNA flow cytometry (Fig. 7). As expected, the cell-cycling phases showed no significant differences between the mutant and control myoblasts at the 0 h time point (immediately after cell synchronization). Significant increases in S-phase populations of PTPLa-deficient myoblasts were observed at the 4 h (42.75%) and 8 h (36.26%) time points compared to the control myoblasts (34.70% and 19.99%, respectively). However, cell populations of the mutant myoblasts in the G_2/M phase became smaller (19.60% and 16.81% at the 4 h and 8 h time points, respectively) compared to the control myoblasts (36.73% and 29.84%, respectively), indicating a compromised G_2/M progression in PTPLa-deficient myoblasts. To further verify the abnormal G_2/M progression in the mutant myoblasts, cells in the M phase were quantified. The mutant myoblasts lost dynamic changes, with only half of the control level's cell populations in M phase (Fig. 8A).

Cyclin D1–cyclin-dependent kinase 4/CDK6 (CDK4/6) and cyclin E2-CDK2 are major regulatory complexes that regulate the checkpoint in the G_0/G_1- to S-phase transition (37, 44). To investigate whether the upregulation of these complexes occurred in PTPLa-deficient myoblasts, immunoblot analysis of individual cyclins and CDKs was performed. As indicated in Fig. 8B and C, the cyclin D1, CDK4, CDK6, and cyclin E2 expression levels were markedly increased in the mutant myoblasts compared to the control cells. This suggested that the PTPLa expression level was critical for G_1/S phase transition and that the PTPLa deficiency facilitated the G_1/S-phase transition. The PTPLa-deficient myoblasts also displayed an abnormal G_2/M progression. Since CDK1 is a key regulator of the G_2-to-M-phase transition and the regulation of CDK1 activity involves phosphorylation and dephosphorylation of the kinase, the phospho-CDK1 level was assessed by Western blot analysis. As indicated in Fig. 8D, hyperphosphorylation of CDK1 was detected in the mutant myoblasts along with the upregulation of Myt1, indicating that an inactive CDK1 may contribute to the restrained G_2-to-M transition. Enhanced activity of cyclin/CDK could deregulate DNA replication and cause DNA damage leading to cell death (7), which may potentially contribute to the PTPLa mutant cell growth retardation. To rule out this possibility, we conducted terminal deoxynucleotidyltransferase-mediated dUTP-biotin nick end labeling (TUNEL) and caspase activity assays, which displayed no significant increase in cell death in the mutant myoblasts (data not shown). Finally, we demonstrated the mutant cell cycle defects by double-thymidine-synchronization treatment. Consistent with the low-serum synchronization result, a larger population of cells in the S phase, along with the smaller numbers of cells in the G_2/M phase, was observed in the mutant myoblasts after 4-h and 8-h release from thymidine blocks compared to the wild-type control myoblast results (Fig. 9A). In line with the higher percentage of cells in the S phase, the mutant myoblasts displayed higher BrdU-positive cell numbers in comparison with the control cells (Fig. 9B). Meanwhile, the expression of p21 protein, a cyclin-dependent kinase inhibitor, was increased in the mutant myoblasts at the 0 and 4 h time points after the cell release from thymidine blocks, indicating a potential mechanism and further supporting the finding regarding the cell cycle arrest phenotype in the mutant cells (Fig. 9C). Taken together, these data suggested that the upregulation of cyclin D1 and cyclin E2 complexes, along with the inactivated CDK1 and upregulated p21, might have been responsible for the PTPLa deficiency-mediated S-phase arrest that contributed to the impeded cell growth.

PTPLa is a direct SRF gene target. Serum response factor is essential for skeletal- as well as cardiac- and smooth-muscle gene expression (40, 41, 49). Mice with an SRF deletion in skeletal muscle experienced a severe deficiency in skeletal muscle growth and improper maturation (40). Using computational biology approaches (Genomatix), we analyzed the 5-kb sequence upstream of the PTPLa gene and identified three putative SRF binding sites: SRE1 (serum response element 1), SRE2, and SRE3 (Fig. 10A). The SRE consensus sequence is $CC(A/T)_6GG$, with an AT-rich core. To determine whether SRF binds to the identified SREs, an EMSA was performed. Three ^{32}P-labeled DNA duplexes containing SRE1, SRE2, and SRE3 were used as probes (14). A strong band shift was observed only when the SRE3 probe was incubated with the nuclear extract, and no shift was observed for SRE1 or SRE2 probes (Fig. 10B). This suggested that SRF may bind to the PTPLa promoter via the SRE3. To verify the SRF-SRE3 interaction, a comprehensive EMSA was conducted (Fig. 10C). As expected, a band shift was displayed with the addition of the wild-type SRE3 and nuclear extract (lane 3), while no SRF binding to the mutant SRE3 probe was observed, thus validating the binding specificity (lane 4). A supershift band was obtained by adding an anti-SRF antibody (lane 5), confirming the SRF-SRE3 interaction. Finally, an excess of unlabeled wild-type SRE3 probe was included in the SRF-SRE3 binding reaction, which resulted in the abolishment of

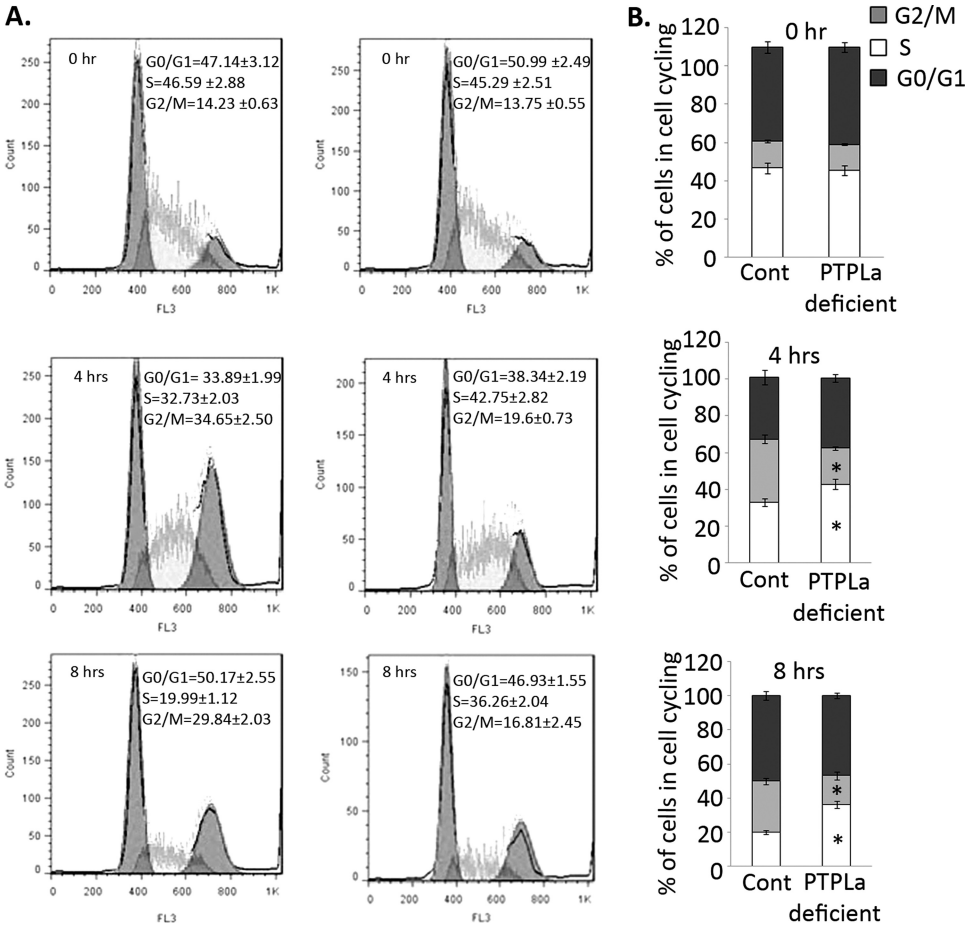

FIG 7 PTPLa knockdown resulted in S-phase arrest in myoblasts. (A) Flow cytometry analysis revealed the impeded S phase and attenuated G_2/M phase in PTPLa-deficient myoblasts. (B) Cell population distribution in cell cycle. The h 0, 4, and 8 time points indicate the periods of time during which the synchronized cells were cultured in the serum restoration growth medium. The data represent the averages of the results of experiments repeated three times with means ± standard errors. *, $P < 0.01$ compared to control (Cont).

the SRF-SRE3 band shift (lane 6). This experiment confirmed that SRF is able to bind the SRE motif in the PTPLa promoter region *in vitro*.

To investigate whether SRF interacts with the PTPLa promoter region *in vivo*, a ChIP assay was performed (66). The specific SRF-DNA complex was immunoprecipitated using an anti-SRF antibody. Sequencing analysis showed that the DNA fragments isolated in the complex contained part of the PTPLa 5′-upstream sequence with the SRE3 site (Fig. 10D). Thus, the *in vivo* interaction of SRF with the SRE3 site in the PTPLa promoter region was confirmed.

To explore the functional significance of SRE3, a 5-kb-long duplex of the PTPLa 5′-upstream sequence containing the SRE3 site was subcloned into a luciferase reporter vector. The chimeric vector can express luciferase as a reporter under PTPLa promoter control. The effect of SRF on luciferase expression can be detected from the changes in luciferase activity. We cotransfected the SRF-expressing vector, and the introduction of SRF increased luciferase activity more than 5-fold compared to the baseline control without SRF (Fig. 10E). In a parallel experiment, the proactive effect of SRF on the PTPLa promoter was completely abolished by the mutation of SRF binding site SRE3 in the PTPLa promoter. This result strongly suggests that the PTPLa is regulated by SRF.

To further demonstrate that PTPLa is one of the SRF direct-target genes, we evaluated PTPLa expression in skeletal muscle from skeletal-muscle-specific SRF deletion mice by the use of a conditional SRF allele harboring loxP sites ($SRF^{loxp/loxp}$) flanking SRF exon 1 (64). Skeletal-muscle-specific SRF deletion was achieved by using a MCK-Cre transgene that has been shown to be activated in skeletal-muscle cells to delete the $SRF^{loxp/loxp}$ allele (12, 40). Skeletal muscle extracted from postnatal day 2 mice was assessed. Based on the Western blot analysis, we estimate that the MCRK-Cre transgene directed deletion of at least 90% of SRF in skeletal muscle (Fig. 11A). PTPLa protein and mRNA levels were then evaluated by Western blot analysis, regular reverse transcription-PCR (RT-PCR), and QPCR (Fig. 11A, B, and C). The results showed marked decreases in PTPLa protein and mRNA expression levels in mutant animal skeletal muscle compared to wild-type animals, suggesting PTPLa as one of SRF regulatory genes.

Most transcription regulatory mechanisms are highly conserved. Because PTPLa is highly expressed in both skeletal muscle and heart tissues, we asked whether the SRF regulation of PTPLa expression was also active in the heart. An inducible αMHC-MerCre transgene was used to delete the $SRF^{loxp/loxp}$ allele (57), and based on the Western blot analysis, the SRF protein level in the

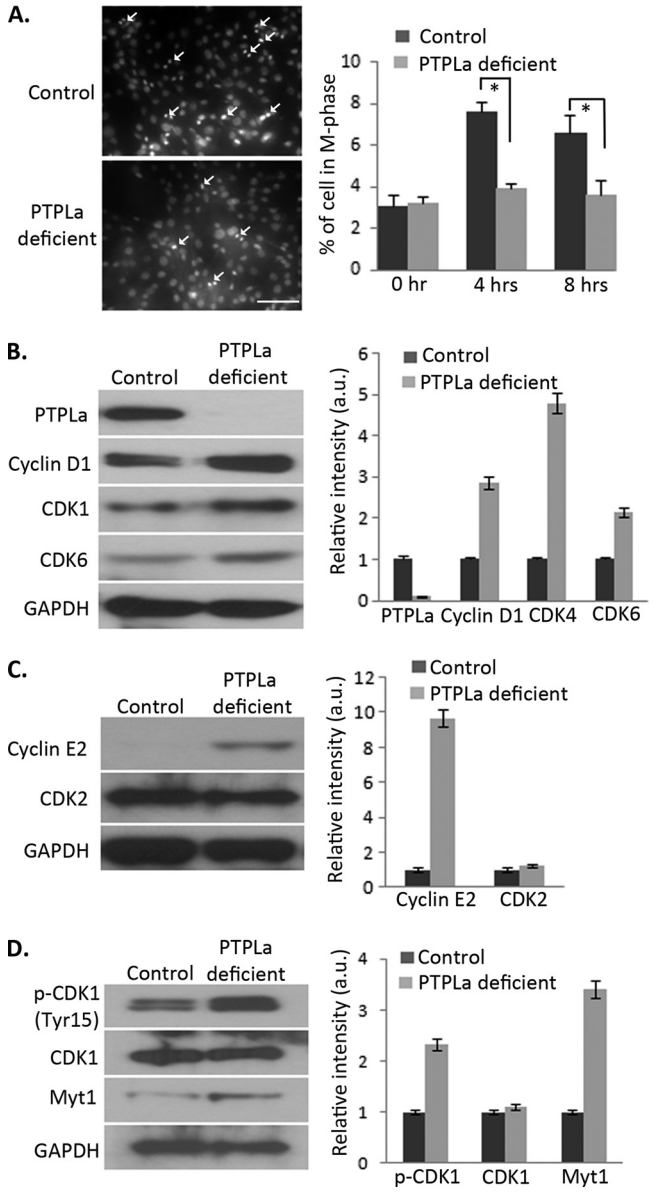

FIG 8 Cell cycle checkpoint dysregulation in PTPLa-deficient myoblasts. (A) A dynamic change in the M-phase cell population was lost in the mutant myoblasts. The h 0, 4, and 8 time points indicate the periods of time during which the synchronized cells were cultured in the serum restoration growth medium. (B and C) Western blots (left panels) showed upregulation of cyclin D1-CDK4/6 and cyclin E2-CDK2 regulatory complexes in the mutant myoblasts. (D) Hyperphosphorylated CDK1, along with upregulation of Myt1, was detected in the mutant myoblasts by Western blot analysis (left panels). (B, C, and D) The right panels display the results of blot densitometry analyses derived from the associated blots shown in the corresponding right panels. Data represent the averages of the results of three measurements from three repeated experiments, with normalization using GAPDH. *, $P < 0.01$ compared to control. Bar, 100 μm. a.u., arbitrary units.

heart was reduced by more than 90% (Fig. 11D). Along with the decrease in SRF expression, significant reductions in PTPLa protein and mRNA levels were also observed (Fig. 11D, E, and F), which was consistent with the observations of skeletal muscle. The result revealed a conserved regulatory mechanism in PTPLa gene expression.

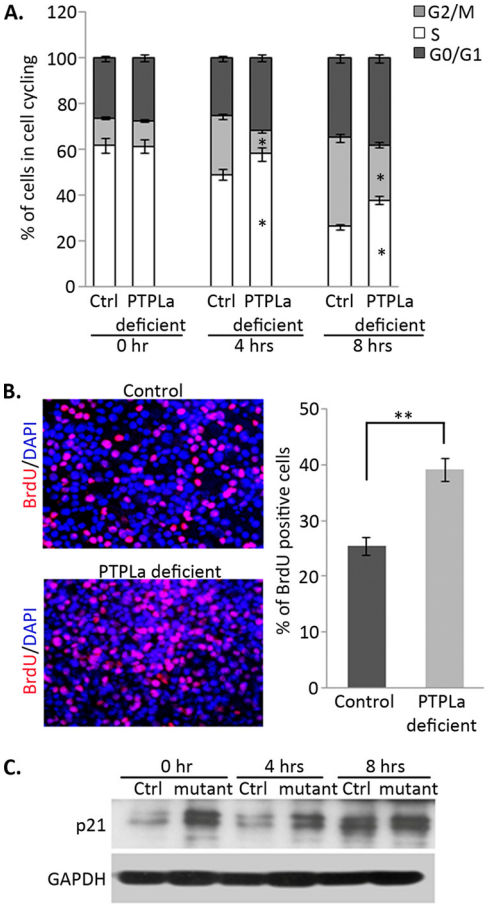

FIG 9 The PTPLa deficiency-mediated cell cycling defect was assessed in cells with double-thymidine synchronizations. (A) Impeded S phase and attenuated G_2/M phase in PTPLa-deficient myoblasts were detected by flow cytometry analysis after double-thymidine blocks followed by 4- and 8-h blockage releases, respectively. The data represent the averages of the results of three repeated experiments. *, $P < 0.05$ compared to the control (Ctrl) results from the indicated time points. (B) The number of BrdU-positive cells (pink) was assessed at the 4-h time point after the thymidine blockage release and was higher in PTPLa-deficient myoblasts than in the control cells. BrdU-positive cells were quantified from nine images taken from three slides (right panel). **, $P < 0.01$. (C) Western blot analysis showed upregulated p21 protein expression in PTPLa-deficient myoblasts (mutant).

DISCUSSION

Emerging evidence reveals that protein tyrosine phosphatases are involved in regulation of skeletal-muscle myogenesis (18, 22–24, 27, 32–34, 42, 60). For example, mutations in myotubularin 1, a PTPase encoded by the MTM1 (myotubular myopathy) gene in humans, is responsible for X-linked centronuclear myopathy in humans and canines (8, 35, 36). Besides the typical PTPases, a new family of protein tyrosine phosphatase-like (PTPL) genes has been identified (26, 62). PTPL proteins have a conserved PTPase catalytic motif, (I/V)HCXXGXXP(S/T), except for the substitution of proline (P) for arginine (R). The biological consequence of the variation is unclear. One recent study in PTPLb, a member of the PTPL family, showed that the restoration of arginine had a minimal effect on PTPase activity (62). Further enzymatic analysis of PTPL is necessary to understand its biochemical characteristics.

Previously, high expression levels of PTPLa mRNA were de-

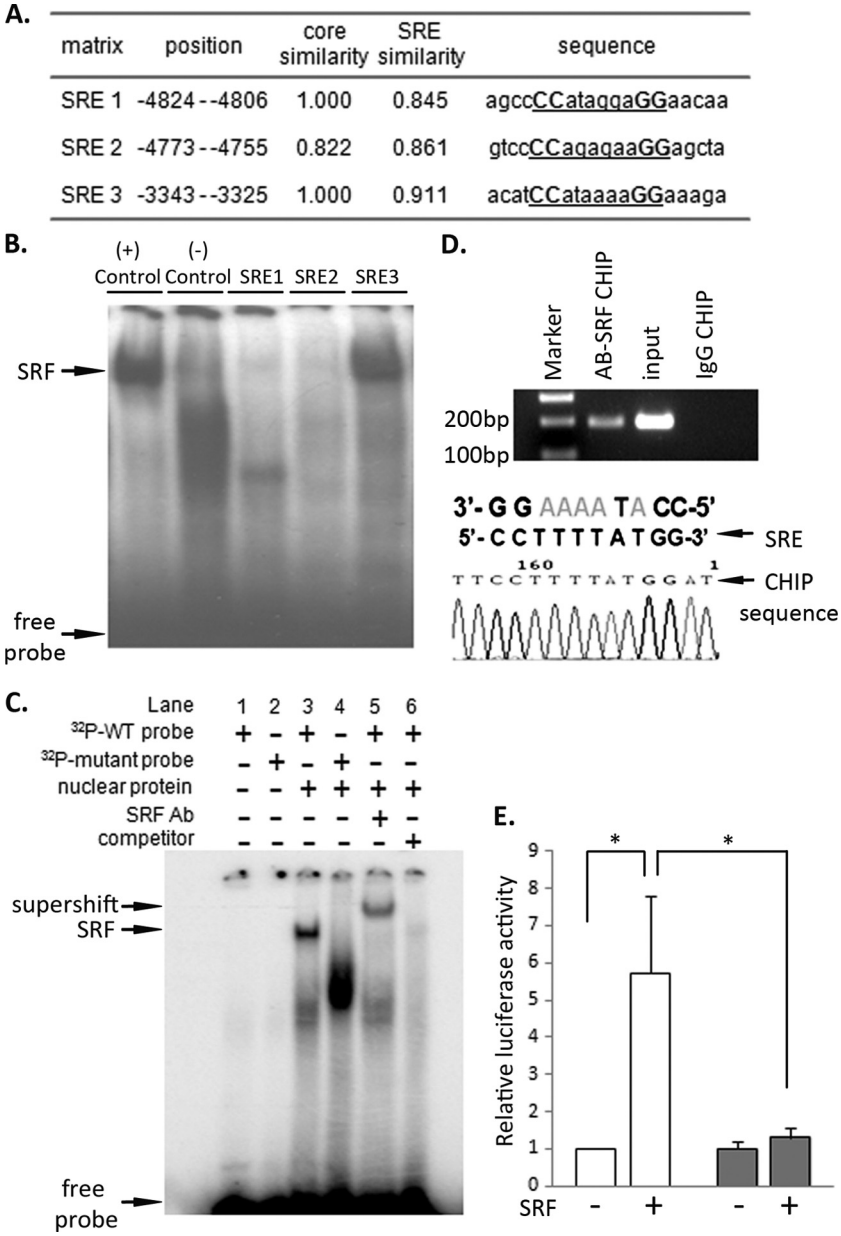

FIG 10 Analysis of PTPLa gene promoter region. (A) Three putative SRF binding sites (SRE1 to SRE3) in the PTPLa gene promoter region were suggested by bioinformatics predictions. (B) Only SRE3 showed interaction with SRF by EMSA. (C) A comprehensive EMSA further demonstrated specific interaction between SRF and the SRE3. (D) A ChIP assay verified their interaction *in vivo*. (E) Addition of SRF activated luciferase activity driven by the PTPLa promoter (empty bars), and mutation of the SRE3 abolished the SRF-mediated reporter activity (gray bars). The data in panel E represent the averages of the results of six measurements, with normalization to the baseline level in the absence of SRF (means ± standard errors). *, $P < 0.01$.

tected in both human and mouse heart- and skeletal-muscle tissues (38, 61). In this study, we found that PTPLa protein was almost exclusively expressed in striated muscles, with the highest protein level detected in mouse heart followed by skeletal muscle, implying its potential role in these tissues. Genetic linkage studies from two independent groups identified PTPLa gene mutations in patients suffering from ARVD (31, 38), although a direct relationship between mutations and disease was not established due to the limitations in human study. Genetically manipulated mouse models such as mutant PTPLa knockin or PTPLa knockout animal models would help define the pathogenic consequences of the presence of mutant PTPLa in heart tissue. Intriguingly, a "natural knockout" PTPLa animal that was due to a SINE (short interspersed repeat element) insertion in the exon of the PTPLa gene was reported in a group of Labrador retrievers. The SINE insertion led to either premature stop or truncated frameshift codons that resulted in PTPLa functional deficiency. The mutant dogs suffered from congenital myopathy with severe hypotonia. Histology analysis revealed centronuclear myopathy along with type 1 fiber atrophy and a type 2 fiber deficiency in skeletal muscle, which closely mimics human autosomal dominant and recessive forms of centronuclear myopathy (52).

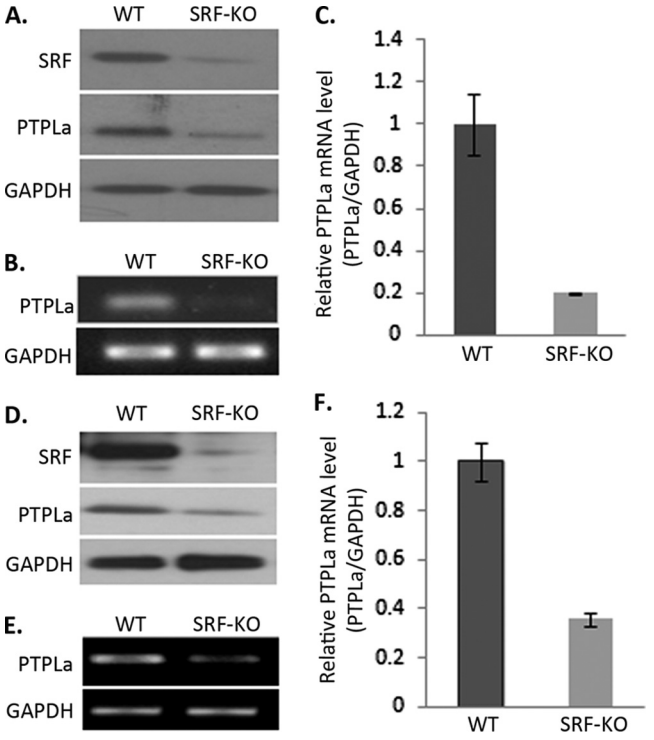

FIG 11 Downregulation of PTPLa expression in SRF-null skeletal and cardiac muscle. (A to C) Skeletal muscle. (D to F) Myocardium. (A and D) Significant decreases in the SRF protein expression were achieved in skeletal muscle- and cardiac-muscle-specific SRF knockout (KO) animals. In parallel with the decline in the SRF expression, repressed PTPLa transcription and protein expression were also detected in the skeletal and cardiac tissues, respectively. (B and E) RT-PCR assay. (C and F) QPCR assay. Data are from four measurements (means ± standard errors).

While all of those previous studies provided strong evidence of PTPLa's function in myogenesis, the underlying molecular mechanism remained unknown. In this study, we identified MyoG as a downstream target of PTPLa. Skeletal myogenesis is tightly orchestrated by members of the MRF family, including MyoD, Myf5, MyoG, and MRF4. MyoD and Myf5 are required for the commitment of proliferating somitic cells to the myogenic lineage, whereas MyoG is required for committed cells (myoblasts) to differentiate into mature myocytes and myotube formation. Targeted disruption of the MyoG gene in mice resulted in perinatal lethality with severe defects in skeletal muscle (25, 48). C2C12 myoblasts proliferate under high-serum conditions and spontaneously differentiate upon serum withdrawal. We observed dramatic increases in MyoD, Myf5, and MyoG expression in C2C12 cells after serum withdrawal; however, the PTPLa deficiency completely blocked the responsive increase in MyoG expression but not in MyoD and Myf5 expression. In parallel with the lack of increase in MyoG expression, the myoblasts lacking PTPLa failed to differentiate and form myotubes. The cells retained the proliferating status even in the serum-free differentiation medium. To understand the relationship between the PTPLa and MyoG, we generated a MyoG-deficient myoblast cell line that (as expected) showed impaired differentiation. By individual rescue experiments, we demonstrated that the introduction of MyoG was sufficient to restore myoblast differentiation in PTPLa-deficient cells and in MyoG-deficient cells. However, introduction of PTPLa rescued the cell differentiation only in PTPLa-deficient cells and not in MyoG-deficient cells. This suggested that PTPLa regulated myoblast differentiation at least partially through MyoG. The next intriguing issue is how PTPLa regulates MyoG. Several early studies demonstrated that MyoG is positively regulated by another essential muscle transcription factor, MEF2 (myocyte enhancer factor 2) (19, 29, 56). We found that MEF2 activity was attenuated in the mutant myoblasts, suggesting possible signaling from PTPLa through MEF2 to regulate MyoG (data not shown).

In this study, we also discovered lower cell growth and DNA synthesis rates in PTPLa-deficient myoblasts. Flow cytometry and immunoblot analyses revealed the S-phase arrest in the mutant cells along with the upregulation of cyclin D and cyclin E complexes. In general, the active complex of cyclin D/CDK4 targets the retinoblastoma protein (pRb) for phosphorylation, allowing the release of E2F transcription factors that activate the G_1/S-phase gene expression (43). Activation of cyclin D/CDK4/6 results in phosphorylation of pRb, which reduces the activity of p21 Waf1/Cip1 and p27 Kip1, allowing subsequent activation of cyclin E/CDK2 (37, 44). Cyclin E/CDK2 further phosphorylates pRb to facilitate the progression into the S phase (21). Therefore, the upregulated cyclin D/CDK4 and cyclin E/CDK2 observed in PTPLa-defective myoblasts enhanced cell entry into the S phase. Meanwhile, the flow cytometry analysis and low growth rate indicated that PTPLa-defective myoblasts failed to divide and to complete the G_2-to-M transition. To reveal a possible mechanism, we analyzed the key regulator in the G_2/M transition, CDK1 (cyclin-dependent kinase 1), encoded by the cdc2 gene in humans. It is well known that dephosphorylation of CDK1 tyrosine-15 and threonine-14 sites activates the kinase and advances cells into mitosis (5, 50). Phosphorylation of CDK1 by Myt1 and Wee1 kinases, however, keeps the CDK1 complex in an inactive state and prevents cells from undergoing the G_2/M transition (45, 63). In PTPLa-deficient myoblasts, hyperphosphorylated CDK1, along with upregulation of Myt1, was observed. Although we do not know whether CDK1 is a direct dephosphorylation target of PTPLa, the impaired G_2/M transition due to PTPLa deficiency strongly implies that this is the case. Furthermore, with the double-thymidine treatments, upregulated p21 expression was observed, suggesting a potential mechanistic role of p21 in PTPLa-mediated cell proliferation regulation. Taking these results together, we believe that the enhanced G_1-to-S entry mediated by upregulation of the cyclin D/CDK4 and cyclin E/CDK2 complexes, along with a compromised G_2/M transition due to the repressed CDK1 activity and upregulated p21, results in cell cycle arrest, which eventually contributes to retarded cell growth.

It is important to realize that, from the biological process point of view, cell proliferation and differentiation are "mutually exclusive" in the sense that differentiation starts when proliferation ceases. However, this does not mean that when one process is impaired the other is necessarily enhanced. In this study, we found that both cell proliferation and differentiation were impaired by PTPLa deficiency through different mechanisms, one operating through cell cycle checkpoint regulation and the other operating through MyoG to regulate differentiation, suggesting that the regulation of myogenesis is complicated, as demonstrated by many earlier studies (40, 58).

Finally, we studied the transcriptional regulation of the PTPLa gene and identified PTPLa as a new target gene for SRF, an essential transcription factor for skeletal-, cardiac-, and smooth-muscle

development. A previous study demonstrated that mouse skeletal muscle lacking SRF expression showed severe hypoplasia and failed to grow (40). SRF directly bound to a DNA sequence known as the serum response element and served as a platform to recruit other muscle regulatory proteins in order to regulate contractile protein gene expression (15, 40, 46, 49, 51). We found that PTPLa regulation by SRF was conserved in both skeletal and cardiac muscle. In mice, the lack of SRF expression in skeletal muscle led to significant decreases in PTPLa transcript and protein expression, which is similar to the phenotype observed in mouse myocardium lacking SRF expression. These results have provided *in vitro* and *in vivo* evidence that SRF transcriptionally regulates the PTPLa gene. Given the fact that SRF functions as a muscle "myogenic driver," it makes sense that PTPLa might be another new downstream target of SRF and that it participates in muscle development.

In summary, the present study defined a promyogenic role of PTPLa, revealed the underlying molecular mechanisms of PTPLa in myoblast proliferation and differentiation, and demonstrated PTPLa gene transcriptional regulation by SRF.

ACKNOWLEDGMENTS

We thank Dafe Uwanogho for the critical discussion on the project. We are grateful to Vladimir N. Potaman and Alexis Boggs for editorial assistance to the manuscript.

This work was supported by the NIH-NHLBI (grants R01HL102314, R21HL094844, and K02HL098956) and by AHA grant-in-aid 0855030F (to J.C.), the NSFC (grants 30860103 and 81060175 to Q.L.), and the National Grant of Basic Research Program of China (grants 2010CB912203 and 2011CB915504 to D.H.).

REFERENCES

1. **Adham IM, et al.** 2005. The scoliosis (sco) mouse: a new allele of Pax1. Cytogenet. Genome Res. **111**:16–26.
2. **Agnati LF, et al.** 2006. Allosteric modulation of dopamine D2 receptors by homocysteine. J. Proteome Res. **5**:3077–3083.
3. **Arnold SR, et al.** 2006. Changing patterns of acute hematogenous osteomyelitis and septic arthritis: emergence of community-associated methicillin-resistant Staphylococcus aureus. J. Pediatr. Orthop. **26**: 703–708.
4. **Arsenian S, Weinhold B, Oelgeschlager M, Ruther U, Nordheim A.** 1998. Serum response factor is essential for mesoderm formation during mouse embryogenesis. EMBO J. **17**:6289–6299.
5. **Atherton-Fessler S, et al.** 1994. Cell cycle regulation of the p34cdc2 inhibitory kinases. Mol. Biol. Cell **5**:989–1001.
6. **Barnoud R, et al.** 2000. Immunohistochemical expression of WT1 by desmoplastic small round cell tumor: a comparative study with other small round cell tumors. Am. J. Surg. Pathol. **24**:830–836.
7. **Bartkova J, et al.** 2005. DNA damage response as a candidate anti-cancer barrier in early human tumorigenesis. Nature **434**:864–870.
8. **Beggs AH, et al.** 2010. MTM1 mutation associated with X-linked myotubular myopathy in Labrador Retrievers. Proc. Natl. Acad. Sci. U. S. A. **107**:14697–14702.
9. **Berkes CA, Tapscott SJ.** 2005. MyoD and the transcriptional control of myogenesis. Semin. Cell Dev. Biol. **16**:585–595.
10. **Braun T, Bober E, Winter B, Rosenthal N, Arnold HH.** 1990. Myf-6, a new member of the human gene family of myogenic determination factors: evidence for a gene cluster on chromosome 12. EMBO J. **9**:821–831.
11. **Braun T, Buschhausen-Denker G, Bober E, Tannich E, Arnold HH.** 1989. A novel human muscle factor related to but distinct from MyoD1 induces myogenic conversion in 10T1/2 fibroblasts. EMBO J. **8**:701–709.
12. **Brüning JC, et al.** 1998. A muscle-specific insulin receptor knockout exhibits features of the metabolic syndrome of NIDDM without altering glucose tolerance. Mol. Cell **2**:559–569.
13. **Chang J, Knowlton AA, Wasser JS.** 2000. Expression of heat shock proteins in turtle and mammal hearts: relationship to anoxia tolerance. Am. J. Physiol. Regul. Integr. Comp. Physiol. **278**:R209–R214.
14. **Chang J, et al.** 2003. Inhibitory cardiac transcription factor, SRF-N, is generated by caspase 3 cleavage in human heart failure and attenuated by ventricular unloading. Circulation **108**:407–413.
15. **Chen CY, Schwartz RJ.** 1996. Recruitment of the tinman homolog Nkx-2.5 by serum response factor activates cardiac alpha-actin gene transcription. Mol. Cell. Biol. **16**:6372–6384.
16. **Coolican SA, Samuel DS, Ewton DZ, McWade FJ, Florini JR.** 1997. The mitogenic and myogenic actions of insulin-like growth factors utilize distinct signaling pathways. J. Biol. Chem. **272**:6653–6662.
17. **Davis RL, Weintraub H, Lassar AB.** 1987. Expression of a single transfected cDNA converts fibroblasts to myoblasts. Cell **51**:987–1000.
18. **de Oliveira MV, et al.** 2009. SHP-2 regulates myogenesis by coupling to FAK signaling pathway. FEBS Lett. **583**:2975–2981.
19. **Du SJ, Gao J, Anyangwe V.** 2003. Muscle-specific expression of myogenin in zebrafish embryos is controlled by multiple regulatory elements in the promoter. Comp. Biochem. Physiol. B Biochem. Mol. Biol. **134**: 123–134.
20. **Edmondson DG, Olson EN.** 1989. A gene with homology to the myc similarity region of MyoD1 is expressed during myogenesis and is sufficient to activate the muscle differentiation program. Genes Dev. **3**:628–640.
21. **Ewen ME.** 2000. Where the cell cycle and histones meet. Genes Dev. **14**:2265–2270.
22. **Fornaro M, et al.** 2006. SHP-2 activates signaling of the nuclear factor of activated T cells to promote skeletal muscle growth. J. Cell Biol. **175**: 87–97.
23. **Goel HL, Dey CS.** 2002. Focal adhesion kinase tyrosine phosphorylation is associated with myogenesis and modulated by insulin. Cell Prolif. **35**: 131–142.
24. **Goel HL, Dey CS.** 2002. PKC-regulated myogenesis is associated with increased tyrosine phosphorylation of FAK, Cas, and paxillin, formation of Cas-CRK complex, and JNK activation. Differentiation **70**:257–271.
25. **Hasty P, et al.** 1993. Muscle deficiency and neonatal death in mice with a targeted mutation in the myogenin gene. Nature **364**:501–506.
26. **Healy C, Uwanogho D, Sharpe PT.** 1999. Regulation and role of Sox9 in cartilage formation. Dev. Dyn. **215**:69–78.
27. **Hinard V, Belin D, Konig S, Bader CR, Bernheim L.** 2008. Initiation of human myoblast differentiation via dephosphorylation of Kir2.1 K+ channels at tyrosine 242. Development **135**:859–867.
28. **Huang C, et al.** 2010. Reduction of PKCbetaII activity in smooth muscle cells attenuates acute arterial injury. Atherosclerosis **212**:123–130.
29. **Johanson M, et al.** 1999. Transcriptional activation of the myogenin gene by MEF2-mediated recruitment of myf5 is inhibited by adenovirus E1A protein. Biochem. Biophys. Res. Commun. **265**:222–232.
30. **Kaliman P, Vinals F, Testar X, Palacin M, Zorzano A.** 1996. Phosphatidylinositol 3-kinase inhibitors block differentiation of skeletal muscle cells. J. Biol. Chem. **271**:19146–19151.
31. **Konishi H, Okuda A, Ohno Y, Kihara A.** 2010. Characterization of HACD1 K64Q mutant found in arrhythmogenic right ventricular dysplasia patients. J. Biochem. **148**:617–622.
32. **Kontaridis MI, et al.** 2004. SHP-2 positively regulates myogenesis by coupling to the Rho GTPase signaling pathway. Mol. Cell. Biol. **24**: 5340–5352.
33. **Kontaridis MI, Liu X, Zhang L, Bennett AM.** 2001. SHP-2 complex formation with the SHP-2 substrate-1 during C2C12 myogenesis. J. Cell Sci. **114**:2187–2198.
34. **Koyama T, et al.** 2008. Interaction of scaffolding adaptor protein Gab1 with tyrosine phosphatase SHP2 negatively regulates IGF-I-dependent myogenic differentiation via the ERK1/2 signaling pathway. J. Biol. Chem. **283**:24234–24244.
35. **Laporte J, et al.** 1997. Mutations in the MTM1 gene implicated in X-linked myotubular myopathy. ENMC International Consortium on Myotubular Myopathy. European Neuro-Muscular Center. Hum. Mol. Genet. **6**:1505–1511.
36. **Laporte J, et al.** 1996. A gene mutated in X-linked myotubular myopathy defines a new putative tyrosine phosphatase family conserved in yeast. Nat. Genet. **13**:175–182.
37. **Lauper N, et al.** 1998. Cyclin E2: a novel CDK2 partner in the late G1 and S phases of the mammalian cell cycle. Oncogene **17**:2637–2643.
38. **Li D, Gonzalez O, Bachinski LL, Roberts R.** 2000. Human protein tyrosine phosphatase-like gene: expression profile, genomic structure, and mutation analysis in families with ARVD. Gene **256**:237–243.
39. **Li Q, Lin X, Yang X, Chang J.** 2010. NFATc4 is negatively regulated in

miR-133a-mediated cardiomyocyte hypertrophic repression. Am. J. Physiol. Heart Circ. Physiol. **298**:H1340–H1347.
40. **Li S, et al.** 2005. Requirement for serum response factor for skeletal muscle growth and maturation revealed by tissue-specific gene deletion in mice. Proc. Natl. Acad. Sci. U. S. A. **102**:1082–1087.
41. **Li S, Wang DZ, Wang Z, Richardson JA, Olson EN.** 2003. The serum response factor coactivator myocardin is required for vascular smooth muscle development. Proc. Natl. Acad. Sci. U. S. A. **100**:9366–9370.
42. **Lu H, et al.** 2002. The differentiation of skeletal muscle cells involves a protein-tyrosine phosphatase-alpha-mediated C-Src signaling pathway. J. Biol. Chem. **277**:46687–46695.
43. **Lukas J, Bartkova J, Bartek J.** 1996. Convergence of mitogenic signalling cascades from diverse classes of receptors at the cyclin D-cyclin-dependent kinase-pRb-controlled G1 checkpoint. Mol. Cell. Biol. **16**:6917–6925.
44. **Lundberg AS, Weinberg RA.** 1998. Functional inactivation of the retinoblastoma protein requires sequential modification by at least two distinct cyclin-cdk complexes. Mol. Cell. Biol. **18**:753–761.
45. **McGowan CH, Russell P.** 1993. Human Wee1 kinase inhibits cell division by phosphorylating p34cdc2 exclusively on Tyr15. EMBO J. **12**:75–85.
46. **Miano JM, et al.** 2004. Restricted inactivation of serum response factor to the cardiovascular system. Proc. Natl. Acad. Sci. U. S. A. **101**:17132–17137.
47. **Miner JH, Wold B.** 1990. Herculin, a fourth member of the MyoD family of myogenic regulatory genes. Proc. Natl. Acad. Sci. U. S. A. **87**:1089–1093.
48. **Nabeshima Y, et al.** 1993. Myogenin gene disruption results in perinatal lethality because of severe muscle defect. Nature **364**:532–535.
49. **Niu Z, et al.** 2005. Conditional mutagenesis of the murine serum response factor gene blocks cardiogenesis and the transcription of downstream gene targets. J. Biol. Chem. **280**:32531–32538.
50. **Norbury C, Blow J, Nurse P.** 1991. Regulatory phosphorylation of the p34cdc2 protein kinase in vertebrates. EMBO J. **10**:3321–3329.
51. **Parlakian A, et al.** 2004. Targeted inactivation of serum response factor in the developing heart results in myocardial defects and embryonic lethality. Mol. Cell. Biol. **24**:5281–5289.
52. **Pelé M, Tiret L, Kessler JL, Blot S, Panthier JJ.** 2005. SINE exonic insertion in the PTPLA gene leads to multiple splicing defects and segregates with the autosomal recessive centronuclear myopathy in dogs. Hum. Mol. Genet. **14**:1417–1427.
53. **Quach NL, Biressi S, Reichardt LF, Keller C, Rando TA.** 2009. Focal adhesion kinase signaling regulates the expression of caveolin 3 and beta1 integrin, genes essential for normal myoblast fusion. Mol. Biol. Cell **20**:3422–3435.
54. **Quach NL, Rando TA.** 2006. Focal adhesion kinase is essential for costamerogenesis in cultured skeletal muscle cells. Dev. Biol. **293**:38–52.
55. **Rhodes SJ, Konieczny SF.** 1989. Identification of MRF4: a new member of the muscle regulatory factor gene family. Genes Dev. **3**:2050–2061.
56. **Ridgeway AG, Wilton S, Skerjanc IS.** 2000. Myocyte enhancer factor 2C and myogenin up-regulate each other's expression and induce the development of skeletal muscle in P19 cells. J. Biol. Chem. **275**:41–46.
57. **Sohal DS, et al.** 2001. Temporally regulated and tissue-specific gene manipulations in the adult and embryonic heart using a tamoxifen-inducible Cre protein. Circ. Res. **89**:20–25.
58. **Soulez M, et al.** 1996. Growth and differentiation of C2 myogenic cells are dependent on serum response factor. Mol. Cell. Biol. **16**:6065–6074.
59. **Sun L, Chang J, Kirchhoff SR, Knowlton AA.** 2000. Activation of HSF and selective increase in heat-shock proteins by acute dexamethasone treatment. Am. J. Physiol. Heart Circ. Physiol. **278**:H1091–H1097.
60. **Suryawan A, Davis TA.** 2003. Protein-tyrosine-phosphatase 1B activation is regulated developmentally in muscle of neonatal pigs. Am. J. Physiol. Endocrinol. Metab. **284**:E47–E54.
61. **Uwanogho DA, et al.** 1999. Molecular cloning, chromosomal mapping, and developmental expression of a novel protein tyrosine phosphatase-like gene. Genomics **62**:406–416.
62. **Wang B, Pelletier J, Massaad MJ, Herscovics A, Shore GC.** 2004. The yeast split-ubiquitin membrane protein two-hybrid screen identifies BAP31 as a regulator of the turnover of endoplasmic reticulum-associated protein tyrosine phosphatase-like B. Mol. Cell. Biol. **24**:2767–2778.
63. **Wells NJ, et al.** 1999. The C-terminal domain of the Cdc2 inhibitory kinase Myt1 interacts with Cdc2 complexes and is required for inhibition of G(2)/M progression. J. Cell Sci. **112**(Pt. 19):3361–3371.
64. **Wiebel FF, Rennekampff V, Vintersten K, Nordheim A.** 2002. Generation of mice carrying conditional knockout alleles for the transcription factor SRF. Genesis **32**:124–126.
65. **Wright WE, Sassoon DA, Lin VK.** 1989. Myogenin, a factor regulating myogenesis, has a domain homologous to MyoD. Cell **56**:607–617.
66. **Zhang SX, et al.** 2005. Identification of direct serum-response factor gene targets during Me2SO-induced P19 cardiac cell differentiation. J. Biol. Chem. **280**:19115–19126.